Energy & Environmental Science

Dynamic Article Links

Cite this: *Energy Environ. Sci.*, 2011, **4**, 2435

www.rsc.org/ees

PAPER

Photocurrent generation by photosystem 1 integrated in crosslinked redox hydrogels†

Adrian Badura,[a] Dmitrii Guschin,[b] Tim Kothe,[a] Marta J. Kopczak,[a] Wolfgang Schuhmann*[b] and Matthias Rögner*[a]

Received 4th February 2011, Accepted 3rd June 2011
DOI: 10.1039/c1ee01126j

Photosystem 1 (PS1) catalyzes the light driven translocation of electrons in the process of oxygenic photosynthesis. Isolated PS1 was immobilised on a gold electrode surface *via* an Os complex containing redox polymer hydrogel which simultaneously is used as immobilisation matrix and as electron donor for PS1. On addition of methyl viologen as sacrificial electron acceptor, a catalytic photocurrent with densities of up to 29 μA cm^{-2} at a light intensity of 1.8 mW cm^{-2} was observed upon illumination—equivalent to an incident photon to carrier efficiency (IPCE) of 3.1%. The strong dependence of the catalytic reaction on the light intensity and the dissolved oxygen concentration indicates that a significant photocurrent from excited PS1 to the electrode can only be realized in the presence of oxygen.

Introduction

Photosystem 1 (PS1) represents the largest transmembrane multisubunit protein complex in nature and contributes to solar energy conversion in the process of oxygenic photosynthesis. It catalyzes the translocation of electrons from plastocyanin (or cytochrome c_6) on the luminal side to ferredoxin (or flavodoxin) on the cytoplasmic side of the thylakoid membrane. The driving force for this endergonic reaction is supplied by the absorption of visible light by PS1 resulting in a strong change in its redox potential from +0.43 V to −1.3 V of the electron donor P_{700}.

Further electron transfer is realized by a series of cofactors (A_0, A_1, F_X, F_A, F_B), with decreasing redox potentials.[1–3] Altogether the redox potential difference between the P_{700} donor and the F_B acceptor site is about 1 V. The quantum efficiency of the charge separated state P_{700}^+/F_B^- approaches remarkably 100%.[4] These unique photocatalytic properties make PS1 a suitable protein for the conversion of visible light into chemical energy by means of specifically designed bio-electrochemical devices.[5]

The integration of redox enzymes into such devices demands the design of an appropriate electron transfer (ET) pathway between the immobilised protein complex and the electrode surface in order to establish an efficient electrochemical communication. In PS1, reduction and oxidation of the redox

[a]*Plant Biochemistry (Faculty of Biology & Biotechnology), Ruhr-Universität Bochum, Universitätsstrasse 150, D-44780 Bochum, Germany. E-mail: Matthias.roegner@rub.de; Fax: +49 2343214322; Tel: +49 2343223634*

[b]*Analytische Chemie—Elektroanalytik & Sensorik (Faculty of Chemistry & Biochemistry), Ruhr-Universität Bochum, Universitätsstrasse 150, D—44780 Bochum, Germany. E-mail: wolfgang.schuhmann@rub.de; Fax: +49 2343214683; Tel: +49 23432201*

† Electronic supplementary information (ESI) available: See DOI: 10.1039/c1ee01126j

Broader context

Photosynthetic enzymes represent efficient converters for the energy of visible light into storable chemical energy. Within the field of bioelectrochemistry, especially photosystem 1 (PS1) became recently an attractive model compound for energy sourcing. The efficiency of such bioelectrochemical devices depends decisively on the combination of immobilisation procedures with the design of appropriate electron transfer pathways between isolated enzymes and a conductive support. As reduction and oxidation of the redox partners occur on opposite sites of the PS1 complex, the communication with the conductive support has to be realized with at least two suitable redox compounds, *i.e.* donor and acceptor. Previous studies used only freely diffusing electron donors which resulted in a rather low current response of the immobilised enzyme. Here we report on the integration of PS1 into a bioelectrochemical device using osmium-modified redox polymers: they both act as three-dimensional immobilisation matrix and as electron donor. With this simple and rapid drop coating procedure we were able to increase the current response of immobilised PS1 by at least one order of magnitude in comparison with former studies.

This journal is © The Royal Society of Chemistry 2011

partners occur on opposite sides of the complex which are additionally separated by the thylakoid membrane. Thus, the charge separation is nearly irreversible and the electron transfer pathway is sterically predefined to attain a maximum yield of photogenerated products and hence maximum energy storage. However, if the protein is not isotropically orientated within a lipid bilayer membrane both recombination and a short circuit of the redox partners and/or PS1 have to be avoided.

Faulkner *et al.*[6] reported the orientated immobilisation of PS1 on thiolated gold surfaces by vacuum adsorption. The immobilised PS1 complexes showed current densities up to 100 nA cm^{-2} using the free diffusing redox mediator 2,6-dichloroindophenol (DCIP) as electron donor and acceptor at the same time. Comparable approaches were reported by Ciesielski *et al.*[7–9] using either nanoporous gold-leaf electrodes or multilayer assemblies; they should increase the amount of PS1 on the electrode surface, but resulted only in an improvement up to 0.4 μA cm^{-2} mW^{-1}. Immobilisation of PS1 *via* components of its acceptor site was realized by Terasaki *et al.*[10,11] The phylloquinone cofactor of PS1 was extracted in order to enable reconstitution on a naphthoquinone modified gold surface of a field effect transistor. Coupling of PS1 with this molecular wire showed current densities of up to 120 nA cm^{-2} mW^{-1}. Recently, Yehezkeli *et al.*[12] reported photocurrents by bis-aniline crosslinked Pt-nanoparticle/PS1 composites crosslinked with ferredoxin on electrodes, reaching current densities of up to 1.38 μA cm^{-2} mW^{-1}. However, these studies suffer from a poor communication between the immobilised PS1 and the electrode surface. Interestingly, nearly all relevant studies used DCPIP as freely diffusing reductant of P_{700}^{+}. As the electron transfer within PS1 occurs in less than 1 μs, theoretical current densities in the mA cm^{-2} range can be expected, based on a PS1 monolayer with assumed 0.5 pMol cm^{-2}.[13,11] Thus, the photocatalytic efficiency of PS1 on electrode surface has to be optimized by either increasing the amount of immobilised protein complex or by improving the ET pathway, *i.e.* its kinetics. Due to the limitation by mass transport to the electrode, this cannot be achieved by DCPIP as electron donor.

However, specifically designed redox polymers showed already a significant increase of both current density and long-term stability[14] with photosystem 2 (PS2) complexes immobilised on electrode surfaces. Also, redox polymers have been successfully applied previously for the development of reagentless biosensors.[15–19] The redox polymers are simultaneously used as immobilisation matrix and as a polymeric ET mediator for the polymer-integrated biological recognition element, typically a redox enzyme. ET from the active site of the enzyme to the electrode surface occurs *via* a sequence of self-exchange reactions along neighbouring redox centers, which are covalently or coordinatively bound to the polymer backbone.[20] Parameters such as the polymer backbone, the ET distance and formal potential of the polymer-bound redox centers contribute to the performance of related biosensors.[21–23]

Here, we report on the immobilisation of PS1 isolated from *Thermosynechococcus elongatus* on gold electrodes using different Os complex modified redox polymers as immobilisation matrix and non-diffusible electron donors for PS1. Light induced ET of PS1 was studied with regard to light intensity, quantum efficiency and O_2 concentration.

Experimental

Isolation of PS1 trimers from *Thermosynechococcus elongatus*

The thermophilic cyanobacterium *T. elongatus* was cultivated in BG11 medium, harvested and disrupted for thylakoid membrane isolation using a Parr bomb according to ref. 24. After repeated homogenization in buffer A (20 mM HEPES pH 7.5, 0.5 M mannitol, 10 mM $MgCl_2$ and 10 mM $CaCl_2$) at a chlorophyll concentration of about 1 mg mL^{-1}, thylakoid membranes were centrifuged (20 min at 9000 *g*) and washed three times with this buffer containing 0.05% *n*-dodecyl-β-D-maltoside (β-DM, Biomol, Germany) to remove the membrane attached antenna complexes (phycobilisomes). Extraction of PS1 from the resuspended membranes started with a high-salt incubation under 20 min continuous stirring at 50 °C (20 mM HEPES pH 7.5, 10 mM $MgCl_2$ and 10 mM $CaCl_2$, 200 mM ammonium sulfate), followed by addition of β-DM (1.0%) and 20 min continuous stirring at room temperature. Solubilized PS1 was harvested by ultracentrifugation (1 h at 180 000 *g*).

Chromatographic purification was performed on the PerSeptive Biocad 700 E chromatography system (Applied Biosystems), starting with a hydrophobic interaction chromatography step on a POROS 50–OH column (Applied Biosystems). For this, the filtrated (0.45 μm membrane) supernatant of the ultracentrifugation step was supplemented by 1.5 M ammonium sulfate and loaded onto the equilibrated (buffer A with 1.5 M ammonium sulfate and 0.03% β-DM) column. After column washing the bound complexes were eluted by two gradient steps (from 1.5 to 1.1 M and from 1.1 to 0 M) of ammonium sulfate. The eluted PS1 was desalted and/or concentrated by either overnight dialysis at 10 °C (buffer A with 0.025% β-DM), using centricons (MWCO 100 000, Millipore, Germany), or by a combination of both methods. For the second chromatographic step, an Uno Q II ion exchange column (BioRad Laboratories, Germany) was equilibrated with buffer A containing 0.03% β-DM. The concentrated and desalted PS1 of the first column was loaded onto the ion exchange column and eluted by a linear gradient of $MgSO_4$. Purified PS1 complexes were then concentrated and desalted (see above) and stored at −70 °C after snap freezing prior to use.

Synthesis of the redox polymers

Redox polymer P1 was synthesized acc. to Badura *et al.*,[14] polymers P2 and P3 acc. to Guschin *et al.*[25]

Electrode modification

Prior to modification, gold electrodes ($Ø$ = 2 mm, CH-Instruments, USA) were cleaned by polishing with alumina oxide paste (down to 0.3 μm grain size, Leko, Germany). After rinsing with water, the electrodes were electropolished in 0.5 M H_2SO_4 (Sigma-Aldrich, Germany) by cycling between −100 mV and +1500 mV at a scan rate of 100 mV s^{-1} for 20 cycles. Electrodes were modified using 2 mg mL^{-1} PS1 in buffer (20 mM HEPES with 0.03% [w/v] β-DM), 8 mg mL^{-1} redox polymer and 1 mg poly(ethylene glycol)diglycidyl ether (PEGDGE, Polyscience, USA) dissolved in distilled water (stock solution of 20 μL PS1, 3 μL polymer solution and 1 μL PEGDGE, manual mixing). A 4 μL droplet was deposited by a pipette on the surface of a 2 mm

 This journal is © The Royal Society of Chemistry 2011

gold disc electrode, followed by 24 h dark incubation at 4 °C to induce cross-linking by PEGDGE. Prior to use, electrodes were washed with buffer solution containing 10 mM Na-citrate pH 5.5, 10 mM $MgCl_2$, 10 mM $CaCl_2$ and 0.03% [w/v] β-DM to remove loosely bound compounds.

Electrochemical instrumentation

Electrochemical measurements were done with an AUTOLAB PGSTAT 12 potentiostat (Eco Chemie, Netherlands), using gold disk working electrodes with an Ag/AgCl reference electrode (WPI, USA) and 3.5 M KCl as internal electrolyte. Home-made platinum electrodes had a diameter of 1 mm. Differential pulse voltammetry of the Os complex modified polymers was done using a three-electrode set-up: a 1 mm platinum disk electrode as working electrode, a Ag/AgCl reference electrode and a Pt wire as counter electrode. Prior to measurements, the Pt disk electrodes were polished using a polishing cloth with decreasing size of alumina paste (3 μm, 1 μm, 0.3 μm) and ultrasonicated in water for 5 min.

Electrochemical experiments with immobilised PS1 complexes were carried out at 25 °C in a buffered electrolyte containing Na-citrate (pH 5.5), 10 mM $MgCl_2$, 10 mM $CaCl_2$, 2 mM 1,1′dimethyl-4,4-bipyridinium (methyl viologen, Sigma-Aldrich, Germany) and 0.03% [w/v] β-DM. Unless otherwise stated, the solution was purged with O_2. The current response of the immobilised PS1 was registered by applying a constant potential of 0 V (unless otherwise stated). Immobilised PS1 was illuminated with a light emitting diode peaking at 680 nm (FAT-685-40, Roithner-Lasertechnik, Austria). In order to avoid warming at higher light intensities, LEDs were cooled down to −16 °C in an ethanol bath. A programmable power supply (PXI-4110, National Instruments, Germany) and a quantum sensor (Li-190, Li-COR Environmental, Germany) were used to adjust the irradiation intensity precisely. Irradiance—in units of power (P) mW cm^{-2} used in this paper—was calculated from the quantum flux μmol photons s^{-1} m^{-2} as indicated by the sensor. Cyclic voltammetry under continuous illumination was recorded under identical conditions as chronoamperometry at a scan rate of 10 mV s^{-1}. In order to monitor the dependence on the generated photocurrent from the light intensity, the LED power was modulated stepwise by a control program developed under Labview 8.6 (National Instruments, Germany). The following parameters were used: range: 0.0036–4.05 mW cm^{-2}; number of data points: 5000; step time: 100 ms. Oxygen saturation within the measuring cell was monitored with a Fibox 1 (PreSens, Germany).

Results and discussion

Immobilisation of PS1 isolated from *Thermosynechococcus elongatus* requires preserving its activity while simultaneously allowing an efficient ET from the active site of PS1 after photoinduced charge separation. Evidently, ET from the co-immobilised electron donor has to be as fast as possible to allow a high photocurrent. Os complex modified redox hydrogels are proposed to fulfill the principle requirements, especially due to the fact that the polymer-bound Os complexes exhibit high stability in both the Os^{2+} and the Os^{3+} states; moreover, they show low reorganization energy and the possibility to tune the redox potential of the polymer-bound Os complexes by modifications in their ligand sphere.[26] For optimal function of PS1 it should be considered that at least two ET mediators are indispensably necessary to enable the envisaged light-induced ET between immobilised PS1 and the electrode surface. Here, we propose Os complex modified hydrogels as electron donors for reducing the photooxidized P_{700}. In addition, at the PS1 acceptor side, F_B is oxidized by methyl viologen (MV) which acts as a sacrificial electron acceptor and further on reduces molecular O_2 to superoxide. The overall reaction sequence is depicted in Fig. 1.

First step is the photogenerated charge separation of the [P_{700}, F_B^-] pair, followed by either MV^{2+} reduction or Os^{2+} oxidation. Both routes are thermodynamically favourable provided the redox potential difference is high enough. Assuming a midpoint potential of −0.785 V (*vs.* Ag/AgCl) for F_B/F_B^-, a ΔE for the acceptor site of 0.155 V ($E^{\circ\prime}(MV^{2+}/MV^{+}) = -0.630$ *vs.* Ag/AgCl) can be derived.[27] In contrast, the formal potential of the P_{700}/P_{700}^+ pair varies from +0.170 to +0.320 V *vs.* Ag/AgCl, in agreement with recent data from spectroelectrochemistry of PS1-trimers of *T. elongatus*, which suggest a formal potential of +0.217 V *vs.* Ag/AgCl.[2]

Taking this into account, three Os complex modified redox polymers were synthesized exhibiting formal potentials of

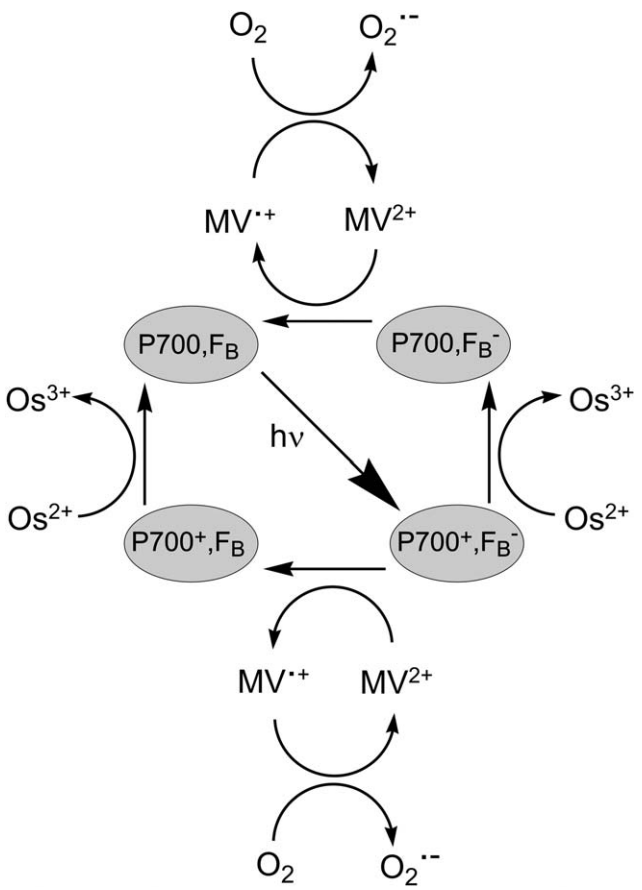

Fig. 1 Reaction sequence of the electron exchange between PS1, Os complexes and methyl viologen. Adapted from ref. 29. For details see text.

$P1 = 0.19$ V, $P2 = 0.293$ V and $P3 = 0.296$ V (*vs.* Ag/AgCl), as derived from the differential pulse voltammograms of redox-polymer modified electrodes (see ESI†). These redox polymers were evaluated with respect to their suitability as electron donors for PS1. While P1 has already been reported as electron acceptor for photosystem 2,[14] P2 and P3 have previously been used with horseradish peroxide in reagentless amperometric biosensors.[25] Immobilisation of PS1 in the polymer matrix is realized by manual mixing of each of the redox polymers with PS1 and the bifunctional crosslinker PEGDGE. Thereafter, a gold disc electrode with an active diameter of 2 mm is modified by drop coating. Chronoamperometry at a constant potential which is sufficiently low to invoke the reduction of polymer-bound Os^{3+} to Os^{2+} was used to monitor the current response of the polymer/PS1 modified electrodes (see Table 1).

Upon illumination of the electrode at a light intensity of 1.8 mW cm^{-2}, the catalytic oxidation of the Os complex modified polymer by PS1 results in a sharp increase of the cathodic current as shown in a typical current response curve (Fig. 2). As summarized in Table 1, all Os complex modified polymers showed high current densities of up to 29 μA cm^{-2} with P1, which are at least one order of magnitude higher than in previously reported systems.[6–12] Interestingly, P2 and P3 are still able to reduce $P700^+$ although their formal potential is at least 76 mV than $P_{700}/P_{700}{}^+$ as determined by spectroelectrochemistry.[2]

Highest photocurrent densities of PS1, however, were observed with polymer P1. In order to correlate this photocurrent with the catalytic oxidation of the Os complexes attached to the polymer, the electrode was characterized by cyclic voltammetry in the dark and under illumination (Fig. 3).

In the dark, a quasi-reversible redox wave of the surface-confined Os complex species can be observed with a peak separation of 0.031 V. This deviation from the theoretical expectation for a surface-bound redox species can be attributed to a diffusional limitation of the counter ions or the kinetic limitation of the self-exchange process between neighbouring Os complexes within the polymer matrix. Upon illumination of the electrode the cathodic current is increased due to the catalytic oxidation of the Os complexes at the redox polymer by PS1. Re-reduction of the Os complexes during the voltammetric scan gives rise to the observed increase and is the photoinduced biocatalytic current. This current reaches a plateau with increasing overpotentials which is evidently due to a limitation of the ET process by electron hopping within the redox polymer or the mass transport limitation of the MV^{2+}.[28] In the presence of O_2 (always O_2-saturated solutions were used) the oxidation of MV^+ at $k = 7.7\ 10^8$ M s^{-1} is supposed to be considerably faster than the second order rate constant for the reduction of MV^{2+} by PS1 ($k \approx 10^6$ M s^{-1}).[28,29] For this reason the dependence of the photocurrent from the O_2 concentration was investigated.

Table 1 PS1 photocurrent response of investigated redox polymers

Polymer	Current density,[a] J/μA cm^{-2}	Applied potential/V *vs.* Ag/AgCl	Formal potential/V *vs.* Ag/AgCl
P1	29 ± 5.3	0	0.19
P2	11 ± 2.8	+0.05	0.293
P3	12 ± 2.5	+0.05	0.296

[a] Current response values are means ± S.D. of 20 independent samples.

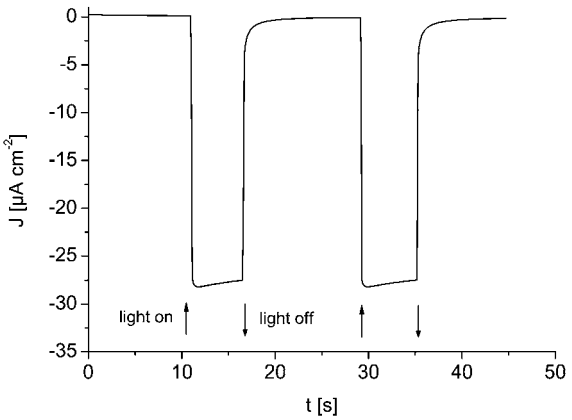

Fig. 2 Current response upon illumination at 680 nm at 1.8 mW cm^{-2} of a gold electrode modified with polymer P1, PS1 and PEGDGE. The supporting electrolyte contains 2 mM methyl viologen as electron acceptor. The applied potential was 0 V *vs.* Ag/AgCl.

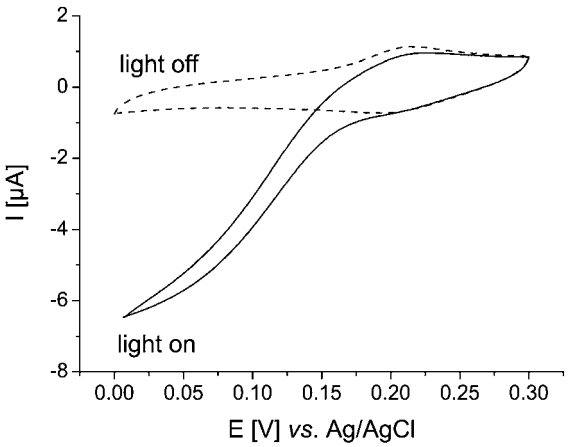

Fig. 3 Cyclic voltammogram of PS1 entrapped within a matrix of the Os complex modified polymer P1 and PEGDGE (dashed line). The solid line represents the cyclic voltammogram from the same electrode upon illumination at 680 nm at a light intensity of 1.8 mW cm^{-2}. Parameters: buffered electrolyte solution: Na-citrate (pH 5.5), 10 mM $MgCl_2$, 10 mM $CaCl_2$, 2 mM 1,1′-dimethyl-4,4-bipyridinium (methyl viologen) and 0.03% [w/v] β-DM; scan rate: 5 mV s^{-1}.

O_2 dependence of the photocurrent

Under continuous illumination and at a constant potential of 0 V (*vs.* Ag/AgCl) the PS1 related photocurrent decreases to zero if the buffer was carefully flushed with Ar to remove any dissolved O_2 (Fig. 4). At the applied potential of 0 V, MV^+ can be directly re-oxidized at the electrode surface leading to a short circuit ($E^\circ(MV^{2+}/MV^+) = -0.63$ V *vs.* Ag/AgCl). Addition of O_2 increases the catalytic current rapidly to a maximum of about 100 nA. Concomitantly, the O_2 concentration in solution increased as monitored by an oxygen sensor. Interestingly, the PS1/Os-polymer modified electrode shows a faster response time towards the presence of O_2 than the O_2 sensor itself. However,

 This journal is © The Royal Society of Chemistry 2011

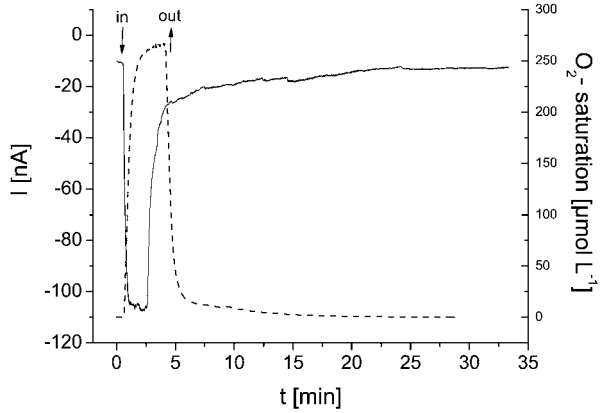

Fig. 4 Chronoamperogram for the elucidation of the dependence of the PS1-based photocurrent on the O_2 concentration in the solution. At the beginning of the experiment the buffer was O_2 free by flushing with Ar. Arrows indicate the time when O_2 was bubbled into the solution (in) or removed again by bubbling with Ar (out). The dashed line shows the O_2 saturation (right axis) as determined by an oxygen sensor.

the data indicate that the observed photocurrent is strongly dependent on either the diffusion of MV^{2+} or the re-oxidation of MV^{+} by O_2, which in turn suggests that the ET from the Os complexes is faster than the reaction at the acceptor site of PS1. This is also evident from the amperometric measurement shown in Fig. 2 in which the current slowly decreases during illumination. As the current reaches the same maximum value during the following illumination period, a degradation of the polymer-entrapped PS1 can be excluded. Due to the high formal potential of the terminal iron–sulfur site F_B/F_B^-, PS1 is in principle able to reduce O_2 in the absence of any freely diffusing electron acceptor such as MV^{2+}.[30] As shown in Fig. 5, the photocurrent response in the absence of MV^{2+} is below 10% of the value as compared with experiments carried out in the presence of MV^{2+}. In the absence of both O_2 and MV^{2+}, however, only a negligible photocurrent is observed, which may be attributed to traces of O_2 in the electrolyte solution.

This role of O_2 as electron acceptor of PS1 so far has been overlooked in studies where PS1 was integrated in bioelectrochemical devices.[6–12] Our experiments indicate that PS1-based photocurrents on conducting supports are always realized if a freely diffusing electron donor, of which reduction at the electrode can be controlled, was added. Thus, the assignment of photocurrents from PS1 to a direct ET from the excited PS1 to an electrode may only be reasonable under complete absence of O_2.

Light intensity dependence

For enzymes, which can be excited by light, the light intensity can be considered as an equivalent to the substrate concentration. Photocurrent generation of immobilised PS1 upon modulation of the light intensity was investigated with an intelligent power supply for a LED. This set-up allows triggering the light intensity with high precision, resulting in a resolution in light intensity of 8.1 µW cm^{-2}. The light scan yields a saturation curve (see Fig. 6) which is indicative of the PS1 kinetics. A linear correlation between the light intensity and the photocurrent is only observed for low light intensities (<0.14 mW cm^{-2}). As the dependence of the light intensity on the generated photocurrent is governed by rate limitation, the Michaelis–Menten equation can be applied. From the Lineweaver–Burk plot (inset Fig. 6) the kinetic parameters $I_{max/app} = 38$ µA cm^{-2} and $K_{M/app} = 1.27$ mW cm^{-2} can be derived. These parameters can be used to quantify further optimizations of the ET pathway within the redox polymer matrix. The saturation curve allows the calculation of the quantum yield as the photon to charge current efficiency (IPCE) according to:

$$\text{IPCE}\ (\%) = (\#\ \text{carriers},\ n)/(\#\ \text{photons},\ N) \times 100$$

This parameter is commonly used to evaluate the properties of solar cells and quantifies the number of charge carriers harvested relative to the number of photons of a given wavelength which hit the solar cell. Plotting IPCE *vs.* illumination intensity (Fig. 7) reveals a self-evident inverse relationship as compared with the light saturation curve. At $K_{M/app}$ an IPCE of 3.1% can be observed. Considering the fact that the quantum efficiency of the charge separated state P_{700}^+/F_B^- approaches 100% (see above),

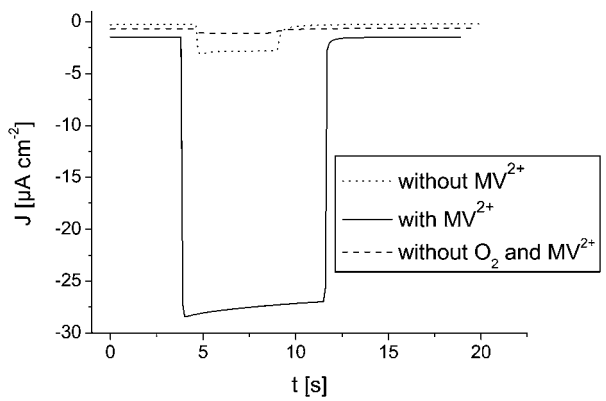

Fig. 5 Photocurrent response of PS1/Os complex modified polymer electrodes upon illumination in the presence of MV^{2+} and O_2 (solid line), in the absence of MV^{2+} (pointed line) and in the absence of MV^{2+} and O_2 (dashed line).

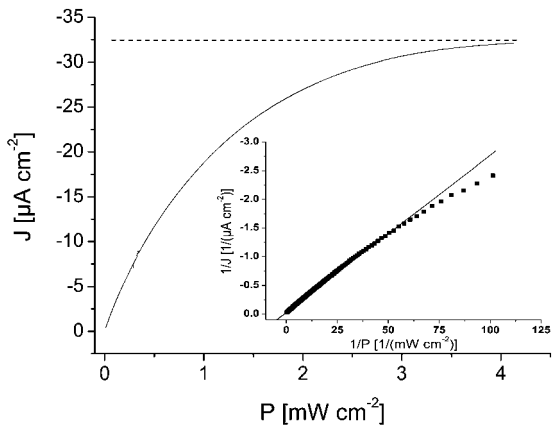

Fig. 6 Light saturation curve of PS1 entrapped within a matrix of polymer P1 and PEGDGE. The inset represents the reciprocal Lineweaver–Burk plot obtained from the saturation curve.

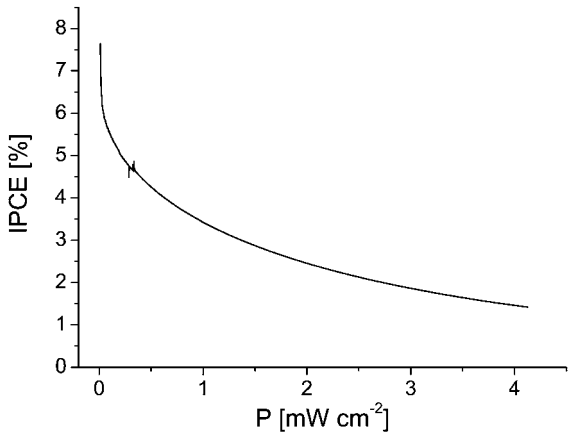

Fig. 7 Relationship between the illumination intensity and the incident photon to current conversion efficiency (IPCE) of immobilised PS1.

this result suggests that further optimization of the device is essential in order to be competitive with—for instance—solar cells. Future investigations should also address long-term stability of immobilised PS1 which involves both the impact of light intensity and the direct environment of PS1, *i.e.* detergent *vs.* lipids.

Conclusions

We propose an easy and time efficient method for the immobilisation of PS1 within cross-linked Os complex modified redox polymers which act as both immobilisation matrix and electron donor. The resulting photocurrent densities of this system (29 μA cm^{-2} at 1.8 mW cm^{-2}) are about one order of magnitude higher than the best values obtained in previous studies with immobilised PS1—strongly indicating that this immobilisation procedure preserves the enzymatic activity of PS1. We suggest that the current is either limited by the diffusion of MV^{2+} or the reoxidation of MV^{+}. For this reason, future studies should address optimization at the acceptor site of PS1—for instance by replacing methyl viologen by a more efficient electron acceptor—in order to achieve an even higher efficiency.

Acknowledgements

Support by the Federal Ministry of Education and Research (BMBF, project H2 design cells; A.B. & M.R.), the EU/NEST project "Solar-H2" (M.R.) and the German Research Foundation (DFG, project C1 in SFB 480; M.R.) is gratefully acknowledged.

Notes and references

1 M. G. Müller, C. Slavov, R. Luthra, K. E. Redding and A. R. Holzwarth, *Proc. Natl. Acad. Sci. U. S. A.*, 2010, **107**, 4123–4128.
2 A. Nakamura, T. Suzawa, Y. Kato and T. Watanabe, *FEBS Lett.*, 2005, **579**, 2273–2276.
3 A. N. Webber and W. Lubitz, *Biochim. Biophys. Acta, Bioenerg.*, 2001, **1507**, 61–79.
4 R. A. Grimme, C. E. Lubner and J. H. Golbeck, *Dalton Trans.*, 2009, 10106–10113.
5 N. Waschewski, G. Bernát and M. Rögner, in *Biomass to Biofuels: Strategies for Global Industries*, ed. N. Q. A. Vertès, H. Blaschek and H. Yukawa, John Wiley& Sons, Ltd., 2010, pp. 387–401.
6 C. J. Faulkner, S. Lees, P. N. Ciesielski, D. E. Cliffel and G. K. Jennings, *Langmuir*, 2008, **24**, 8409–8412.
7 P. N. Ciesielski, C. J. Faulkner, M. T. Irwin, J. M. Gregory, N. H. Tolk, D. E. Cliffel and G. K. Jennings, *Adv. Funct. Mater.*, 2010, **20**, 4048.
8 P. N. Ciesielski, F. M. Hijazi, A. M. Scott, C. J. Faulkner, L. Beard, K. Emmett, S. J. Rosenthal, D. Cliffel and G. Kane Jennings, *Bioresour. Technol.*, 2010, **101**, 3047.
9 P. N. Ciesielski, A. M. Scott, C. J. Faulkner, B. J. Berron, D. E. Cliffel and G. K. Jennings, *ACS Nano*, 2008, **2**, 2465.
10 N. Terasaki, N. Yamamoto, T. Hiraga, Y. Yamanoi, T. Yonezawa, H. Nishihara, T. Ohmori, M. Sakai, M. Fujii, A. Tohri, M. Iwai, Y. Inoue, S. Yoneyama, M. Minakata and I. Enami, *Angew. Chem., Int. Ed.*, 2009, **48**, 1585–1587.
11 N. Terasaki, N. Yamamoto, K. Tamada, M. Hattori, T. Hiraga, A. Tohri, I. Sato, M. Iwai, M. Iwai, S. Taguchi, I. Enami, Y. Inoue, Y. Yamanoi, T. Yonezawa, K. Mizuno, M. Murata, H. Nishihara, S. Yoneyama, M. Minakata, T. Ohmori, M. Sakai and M. Fujii, *Biochim. Biophys. Acta, Bioenerg.*, 2007, **1767**, 653–659.
12 O. Yehezkeli, O. I. Wilner, R. Tel-Vered, D. Roizman-Sade, R. Nechushtai and I. Willner, *J. Phys. Chem. B*, 2010, **114**, 14383–14388.
13 K. Brettel and W. Leibl, *Biochim. Biophys. Acta, Bioenerg.*, 2001, **1507**, 100–114.
14 A. Badura, D. Guschin, B. Esper, T. Kothe, S. Neugebauer, W. Schuhmann and M. Rögner, *Electroanalysis*, 2008, **20**, 1043–1047.
15 K. Habermüller, A. Ramanavicius, V. Laurinavicius and W. Schuhmann, *Electroanalysis*, 2000, **12**, 1383–1389.
16 Y. Ling, M. Haemmerle, A. J. J. Olsthoorn, W. Schuhmann, H. L. Schmidt, J. A. Duine and A. Heller, *Anal. Chem.*, 1993, **65**, 238–241.
17 T. J. Ohara, *Platinum Met. Rev.*, 1995, **39**, 54–62.
18 T. J. Ohara, R. Rajagopalan and A. Heller, *Anal. Chem.*, 1993, **65**, 3512–3517.
19 W. Xu, P. R. Chitnis, A. Valieva, A. van der Est, K. Brettel, M. Guergova-Kuras, Y. N. Pushkar, S. G. Zech, D. Stehlik, G. Shen, B. Zybailov and J. H. Golbeck, *J. Biol. Chem.*, 2003, **278**, 27876–27887.
20 W. Schuhmann, *J. Biotechnol.*, 2002, **82**, 425–441.
21 A. Aoki and A. Heller, *J. Phys. Chem.*, 1993, **97**, 11014–11019.
22 A. W. Bott, *Curr. Sep.*, 2001, **19**, 71–75.
23 R. J. Forster, D. A. Walsh, N. Mano, F. Mao and A. Heller, *Langmuir*, 2003, **20**, 862–868.
24 E. El-Mohsnawy, M. J. Kopczak, E. Schlodder, M. Nowaczyk, H. E. Meyer, B. Warscheid, N. V. Karapetyan and M. Rögner, *Biochemistry*, 2010, **49**, 4740–4751.
25 D. A. Guschin, Y. M. Sultanov, N. F. Sharif-Zade, E. H. Aliyev, A. A. Efendiev and W. Schuhmann, *Electrochim. Acta*, 2006, **51**, 5137–5142.
26 D. Guschin, J. Castillo, N. Dimcheva and W. Schuhmann, *Anal. Bioanal. Chem.*, 2010, **398**, 1661–1673.
27 L. Xiao, G. G. Wildgoose and R. G. Compton, *New J. Chem.*, 2008, **32**, 1628–1633.
28 E. J. Nanni, C. T. Angelis, J. Dickson and D. T. Sawyer, *J. Am. Chem. Soc.*, 1981, **103**, 4268–4270.
29 V. Proux-Delrouyre, C. Demaille, W. Leibl, P. Setif, H. Bottin and C. Bourdillon, *J. Am. Chem. Soc.*, 2003, **125**, 13686–13692.
30 D. C. Goetze and R. Carpentier, *J. Photochem. Photobiol., B*, 1990, **8**, 17–26.

 This journal is © The Royal Society of Chemistry 2011